

FIRST RESULTS FROM ATIC BEAM-TEST AT CERN

O. Ganel¹, J.H. Adams Jr², E.J. Ahn^{7*}, H.S. Ahn¹, J. Ampe², G. Bashindzhagyan³, G. Case⁴, J. Chang⁵, S. Ellison⁴, A. Fazely⁶, R. Gould⁴, D. Granger⁴, R. Gunasingha⁶, T.G. Guzik⁴, Y.J. Han⁷, J. Isbert⁴, T. Kara¹, H.J. Kim⁷, K.C. Kim¹, S.K. Kim⁷, Y. Kwon⁷, T. Lemczyk⁴, C. Oubre⁴, M. Panasyuk³, B. Price⁴, G. Samsonov³, W.K.H. Schmidt⁵, M. Sen⁴, E.S. Seo¹, R. Sina¹, N. Sokolskaya³, M. Stewart⁴, A. Toptygin¹, A. Voronin³, D. Wagner², J.Z. Wang¹, J.P. Wefel⁴, J. Wu¹, V. Zatsepin³, A. Zigura⁴

¹Institute for Physical Science and Technology, University of Maryland, College Park, MD 20742, USA

²Naval Research Laboratory, Washington D.C. 20375, USA

³Skobeltsyn Institute of Nuclear Physics, Moscow State University, Moscow 119899, Russia

⁴Department of Physics and Astronomy, Louisiana State University, Baton Rouge, LA 70803, USA

⁵Max Planck Institut fur Aeronomie, D-37191 Katlenburg-Lindau, Germany

⁶Department of Physics, Southern University, Baton Rouge, LA 70813, USA

⁷Department of Physics, Seoul National University, Seoul 151-742, S. Korea

**Work done while visiting at the University of Maryland*

ABSTRACT

The Advanced Thin Ionization Calorimeter (ATIC) balloon-borne experiment will fly on several 10-day Long Duration Balloon (LDB) flights from McMurdo Station. Its main goal is cosmic ray elemental spectra measurement from 50 GeV to 100 TeV for nuclei from hydrogen to iron. In September 1999 the ATIC detector was exposed to high-energy beams at CERN's SPS accelerator. We will present initial results from these beam-tests, including energy resolutions for electrons and protons at several beam energies from 100 GeV to 375 GeV. Other results to be presented are signal linearity and collection efficiency estimates. We will show how these results compare with expectations based on simulations, and their expected impacts on mission performance.

INTRODUCTION

ATIC (Figure 1) is a balloon-borne experiment to measure the elemental spectra of protons and other nuclei (up to $Z = 26$), for an energy range between about 50 GeV and 100 TeV (Guzik et al., 1999). This is expected to provide hints as to the source of cosmic ray particles, their acceleration mechanism and propagation through the inter-stellar medium.

ATIC is comprised of a fully active bismuth germanate (BGO) calorimeter with ten layers of laterally oriented crystals, each $2.5 \times 2.5 \times 25.0 \text{ cm}^3$. The crystals are held in trays, with 20 crystals in each half-tray for a lateral dimension of $50.3 \times 50.3 \text{ cm}^2$. Small photo-multiplier tubes (PMTs) read out each crystal separately with three dynode pickoffs for

extended linear dynamic range. Above the calorimeter is a 3-layer graphite target shaped as an

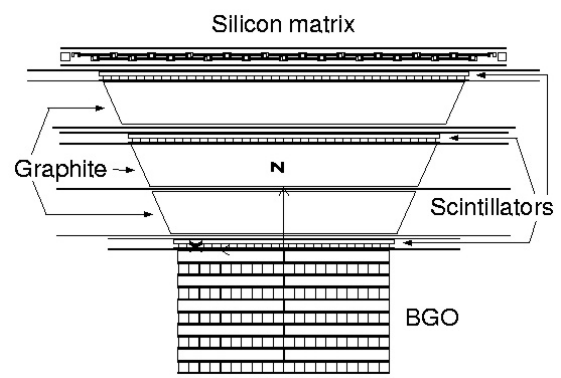


Fig. 1. Simulation model of ATIC configuration

inverted truncated pyramid with a 24° opening angle. Three scintillator strip hodoscopes are located above the target (S1), under the top graphite layer (S2), and above the BGO (S3). Each hodoscope is comprised of a crossed pair of layers with 42 (S1), 35 (S2), or 24 (S3), 2 cm wide, 1 cm thick strips, each read out (2 ranges) from both ends by small PMTs of the same type as used for the BGO. Above the top hodoscope is a matrix of 1.945×1.475 cm² silicon pixels arranged in sets of four pixels per detector, 28 detectors per motherboard, two motherboards per ladder and 20 ladders overall. The Si matrix will cover $\sim 1 \times 1$ m². At the beam-tests only 40 detectors of each of the 3 central ladders were populated.

The calorimeter measures the energy of incident protons and nuclei mostly through the electromagnetic (EM) component of their hadronic shower. The calorimeter depth (about 1.14 nuclear interaction lengths) determines the energy response, i.e. the ratio of measured energy to a particle's incident energy (0.40 – 0.45), as most of the hadronic component of the shower (mainly charged pions) escapes through the bottom and sides of the calorimeter. This also determines the energy resolution ($\sim 35\%$), due to large fluctuations in the fraction of shower energy carried by the EM component. The calorimeter's lateral segmentation allows the reconstruction of the shower axis, pointing back to the primary particle's point of incidence on the Si matrix. The Si matrix is used to measure the incident particle charge (up to $Z = 26$), with its fine segmentation minimizing the impact of back-scattered shower particles on that measurement. The scintillator hodoscopes are used both for triggering (along with BGO signals) and for improving the accuracy of track reconstruction.

BEAM TEST OBJECTIVES AND DATA COLLECTED

As a newly constructed detector, ATIC's hardware and software had to be validated. The energy range ATIC will measure exceeds currently available beam energies by two orders of magnitude, implying how crucial accurate simulations will be for interpreting experimental data. Data from beam tests was thus required to assess the accuracy of ATIC simulations. Additionally, two parameters of critical importance to achieving ATIC's measurement goals, energy resolution and collection efficiency, had to be verified. In September 1999, ATIC was placed in the H2 beamline at CERN's Super Proton Synchrotron (SPS) and collected data from proton, electron and pion beams at energies from 100 GeV to 375 GeV, as well as cosmic muons. Except for cosmic muons, triggered by the ATIC Pre-Trigger, ATIC was triggered externally, using CERN-provided scintillator paddles and trigger electronics to assure passage of precisely one particle per event. This was the first major test of the ATIC hardware and software. Since the beam-test, the ATIC collaboration has been analyzing the data collected at CERN, with the above objectives in mind.

During the one-week run at CERN, ATIC collected data with 150 GeV and 375 GeV protons at 0° , 15° and 30° , in a grid covering much of the calorimeter. Additional runs included 150 GeV negative pions at 0° and 30° , at the center of the device; 100 GeV, 150 GeV and 300 GeV electrons at 0° , 15° and 30° , in a grid similar to the one used for protons; cosmic muons were also recorded with random positions and angles, as were calibration runs (pedestal, charge-pulsar and LED flasher events).

DATA RECORDING AND PROCESSING PROCEDURE

ATIC's Flight Data System (FDS) was used to record the data in binary format on a PC running under the QNX real-time operating system. The data was then transferred to another PC, running under Windows-NT, which served as the Ground Data System (GDS). The data was then transferred to CD-ROMs for processing and analysis. The binary files were read in using a ROOT-based custom package – the ATIC Data Processing System (ADPS). ROOT (Brun and Rademakers, 1997), developed at CERN, is a powerful, object-oriented, data analysis and presentation tool, featuring a C++ interpreter, user-defined classes, dynamic link-in of pre-compiled scripts and a powerful graphical user interface (GUI) with zooming, 3D rotations, detailed inspection of on-screen objects, etc.

A complete mapping between the electronic channels and physical pixels, strips and crystals was used to generate a lookup table linking electronic addresses, physical addresses and exact location for each channel. Using ADPS pedestal values were extracted for each electronic channel and recorded in a pedestal lookup table. Cosmic muon distributions were plotted and fitted for each crystal, strip and pixel to calibrate the Si matrix and the low-range readouts of the calorimeter and scintillator hodoscopes. Events with showers were used to extract the inter-range calibrations for dynode pickoffs. After this calibration, the data was analyzed.

SIMULATIONS

Since 1994, a wide variety of proton showers have been simulated for ATIC using GEANT (Brun et al., 1984). The FLUKA and GHEISHA models were compared, and FLUKA (Arino et al., 1987) was chosen as a more accurate model for the energies of interest to the ATIC experiment. Using GEANT/FLUKA, a detailed ATIC model (Figure 1) has been simulated. Protons were simulated with a variety of energies (including power-law spectra), incident positions and angles (including random position and isotropically distributed angles).

Using these simulations we studied such diverse topics as the number and nature of secondary shower particles, and of back-scattered particles, the energy-deposit pattern from back-scattered particles and its dependence on vertical separation, lateral distance from incident trajectory and target material. Other topics included track reconstruction with BGO information only and with hodoscope and Si matrix information added, the expected charge mis-identification probability in the charge detector vs. energy for different pixel/strip dimensions, determining the first interaction depth, optimization of the ATIC trigger model and a preliminary event selection algorithm, as well as the sensitivity of ATIC to an expected proton spectral break at $\sim 10^{14}$ eV, etc. More recently, based on the run plan, the collaboration simulated the expected beam conditions (particle types, energies, locations and angles) at CERN. These simulations have been used for comparison with the data collected at CERN.

DATA AND SIMULATION RESULTS

Cosmic Muons

Cosmic muon distributions (Figure 2) were used for inter-crystal calibration of the calorimeter's low range readouts and for the low-range of scintillator strips. Absolute calibration was determined by comparing to simulated muons.

Electrons

150 GeV electrons (see Figure 3) were used to validate the overall calibration by comparison to simulated electron showers. Results showed an energy resolution of $\sim 2\%$ at 150 GeV, with 91% containment. Simulated electron events show a similar containment fraction of 92%. The simulated resolution is slightly better due to ideal readout digitization, perfect inter-crystal and inter-range calibrations, etc.

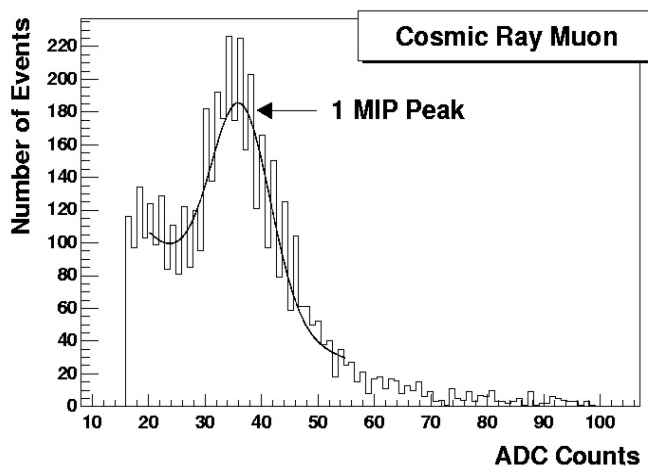


Fig. 2. Typical pedestal subtracted ADC count distribution (with fit) in a BGO crystal due to cosmic muons.

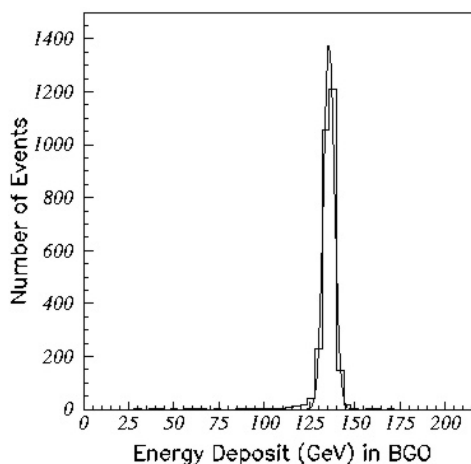


Fig. 3. Total BGO energy deposit (with Gaussian fit) for 150 GeV vertically incident electrons.

Protons

Protons were collected mainly at 150 GeV and 375 GeV. Figure 4 shows a comparison of 150 GeV protons to a (normalized) simulated sample. The two curves are Gaussian and in reasonable agreement (the simulation curve

is slightly narrower for reasons explained in the following section). Figures 5 and 6 below show the longitudinal and lateral profiles of both measured and simulated 150 GeV proton showers. The longitudinal profile comparison shows the simulation accurately reproduces the rising and falling slopes, the overall peak location, and the energy deposited in the lowest calorimeter layers (indicating the leakage fraction) of the experimental measurements. Note that the even layer sums seem, on average, higher than odd layer sums, for both simulation and data. This is due to a set of 3 mm wide steel structural supports located down the middle of each layer. For this data sample, the beam was incident at the center of the calorimeter, but at an angle, such that the trajectory passes near the supports of all odd layers, but not, in general, for even layers. The comparison of lateral profiles shows the simulation reproduces the lateral energy deposit pattern at shower maximum down to less than 1% of the highest single-crystal deposit.

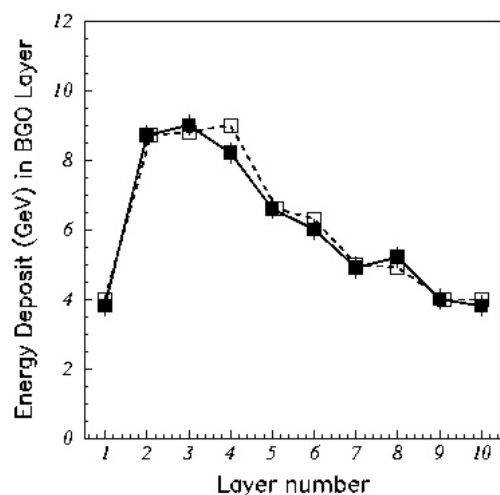


Fig. 5. Longitudinal profile of 150 GeV protons at 30° at center of calorimeter – data (full squares and solid line) and simulation (empty squares and dashed lines).

ATIC'S PERFORMANCE

To correctly interpret flight data and extract the spectral indices of different cosmic ray species (cosmic ray spectra are well-described by power-law distributions over many decades of energy), energy measurements by the ATIC calorimeter should satisfy several requirements. The response should be energy-independent. The reconstructed proton (as well as heavier ion) line-shape should not have non-Gaussian high-end tails, and an energy-independent energy resolution is preferred.

Figure 7 shows the energy (in)dependence of the response and the energy resolution for protons and electrons. The measured response is reproduced well by simulation (proton data 0.43 ± 0.02 vs. simulation 0.44 ± 0.01 , electron data 0.92 ± 0.01 vs. simulation 0.91 ± 0.02). The measured resolutions are compatible with an energy-independent value of $34\% \pm 1\%$ (simulation predicts $29\% \pm 2\%$). The idealized simulation assumes a graphite density of 2.265 g/cm^3 , as opposed to the actual density of 1.76 g/cm^3 of the industrial graphite used by ATIC, thereby increasing the likelihood of secondary shower particles interacting in the target and reducing the fluctuations of the measured signal. The simulation also does not include the multi-range, quantized readout utilized by ATIC to cover the large

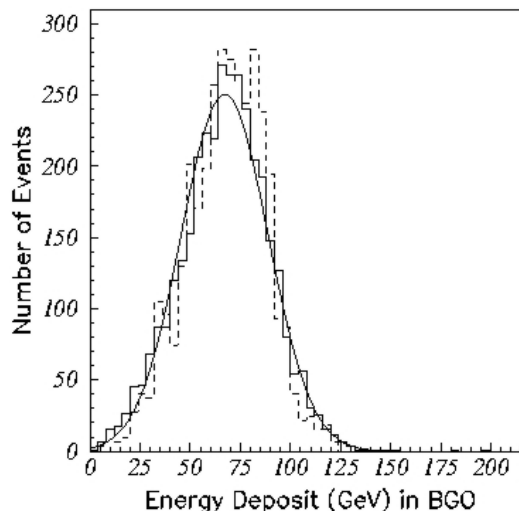


Fig. 4. Total BGO energy deposit for 150 GeV protons at 30° – data (solid histogram and fit) and simulation (dashed histogram)

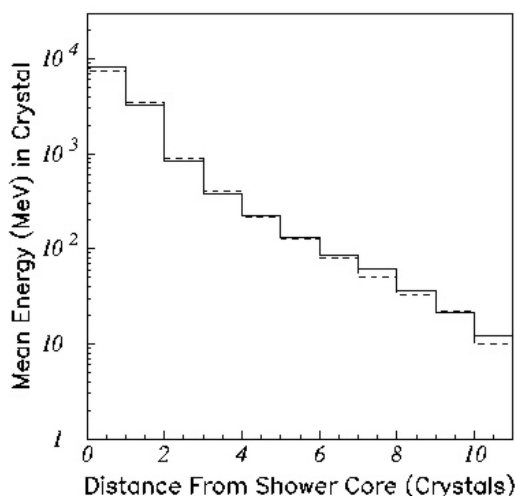


Fig. 6. Lateral profile of 150 GeV protons at 30° at shower maximum – data (solid line) and simulation (dashed line)

dynamic range (about 7 orders of magnitude), and assumes perfect calibration, causing it to under-estimate the uncertainty in energy reconstruction. As shown in Figure 4, the proton line-shape is nicely Gaussian.

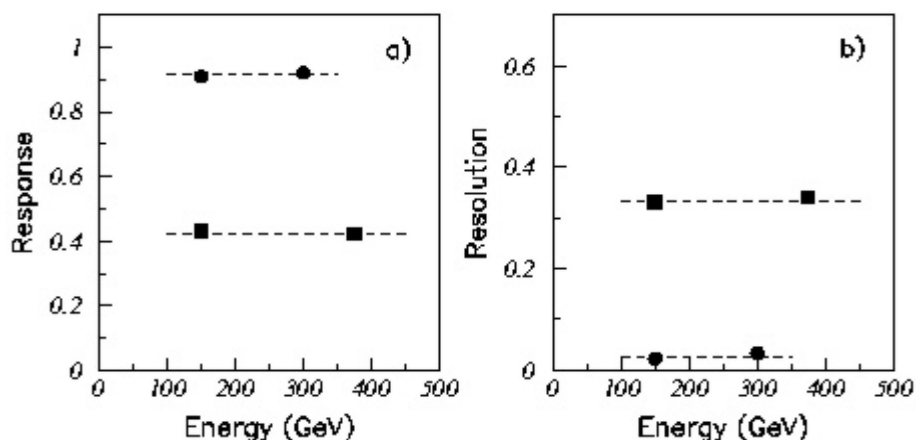


Fig. 7. a) Response vs. incident energy, and b) energy resolution vs. incident energy – protons (squares) and electrons (circles).

Another critical parameter, the collection efficiency will determine the size of the data sample ATIC will be able to collect during its planned flights. With a steeply falling spectrum (the cosmic proton differential flux falls by a factor of 500 for every factor 10 increase in energy in the energy range of interest to ATIC), the highest energy ATIC can reach will be determined by the size of its collected data sample. The collection efficiency is comprised of the probability for the proton to interact in the graphite target, generating a shower, and the likelihood of such a shower event to pass the trigger and event selection. The measured collection efficiency is between 62% (150 GeV) and 66% (375 GeV). Simulations predict a higher efficiency (e.g. 73% at 150 GeV) but accounting for the lower graphite density (see above) that reduces the interaction probability, the prediction drops to 65%, accounting for the difference between simulation and experimental measurement.

CONCLUSIONS

ATIC is expected to fly on its first long duration flight in the winter of 2001, and to measure cosmic ray protons and nuclei from 50 GeV to 100 TeV. To validate the ATIC hardware, software, and simulation, ATIC has taken a large variety of data in a beam test at CERN in September 1999. The energy resolutions, response, collection efficiency, and measured shower profiles agree with simulation results. To the limits of the available beam energies, response and resolution appear energy independent as expected from simulations, with no non-Gaussian high-end tails, promising a successful program. Continued analysis of the beam-test data is expected to yield a great deal of additional valuable information.

ACKNOWLEDGEMENTS

This work was supported by NAG5-5155.

The work done at Moscow State University was supported by the Russian Foundation for Basic Research (grant 99-02-16246) and by the Russian Ministry of Science and Technology.

REFERENCES

- Aarnio, P.A., J. Lindgren, J. Ranft, A. Fassò, and G.R. Stevenson, Enhancements to the FLUKA86 program: (FLUKA87), CERN TIS-RP-190, Geneva, 1987
- Brun, R. and F. Rademakers, ROOT: An Object Oriented Data Analysis Framework, *Nucl. Instr. & Meth.* **A389**, 81-86, 1997
- Brun, R., F. Bruyant, M. Maire, A.C. McPherson, and P. Zancarini, GEANT User's Guide, CERN DD/EE/84-1, Geneva, 1984
- Guzik, T.G., J. Adams Jr., J. Ampe, G. Bashindzhagian, P. Boberg et al., The Advanced Thin Ionization Calorimeter (ATIC) for Studies of High Energy Cosmic Rays, in *Proceedings of the 26th ICRC*, eds. D. Kieda, M. Salamon and B. Dingus, **5**, pp 9-12, Salt Lake City, 1999